Porphyrinoids

Deutsche Ausgabe: DOI: 10.1002/ange.201606293
Internationale Ausgabe: DOI: 10.1002/anie.201606293

# Pictet–Spengler Synthesis of Quinoline-Fused Porphyrins and Phenanthroline-Fused Diporphyrins

*Ke Gao, Norihito Fukui, Seok Il Jung, Hideki Yorimitsu,* Dongho Kim,* and Atsuhiro Osuka**

***Abstract:*** *Doubly and quadruply quinoline-fused porphyrins were effectively synthesized through a reaction sequence consisting of Suzuki–Miyaura coupling of β-borylated porphyrins with 2-iodoaniline and subsequent Pictet–Spengler cyclization. These quinoline-fused porphyrins display red-shifted absorption bands and higher electron-accepting abilities. This synthetic protocol also allowed the synthesis of phenanthroline-fused porphyrin dimers, which bound either a $Ni^{II}$ or $Zn^{II}$ cation. The resultant metal complexes displayed further red shifted absorption spectra and molecular twists to effect an almost perpendicular arrangement of the two porphyrins.*

Porphyrins fused with external aromatic segments and their oligomeric arrays[1] are promising in a wide range of applications such as near-infrared dyes,[2] dye-sensitized solar cells,[3] two-photon absorbing dyes,[4] and organic light-emitting diodes.[5] In addition, porphyrins fused with nitrogen-containing heteroarenes are interesting as structural motifs for nitrogen-incorporated molecular graphene mimics. Syntheses of these arene-fused porphyrins have been so far achieved mostly through oxidative ring closure,[2,6] palladium-catalyzed intramolecular C–H arylations,[7] condensation reactions of arene-fused pyrroles,[8] and retro-Diels–Alder reactions.[9] As an alternative method, acid-catalyzed condensation reactions are useful for the synthesis of such heteroarene-fused porphyrins, as demonstrated by the pioneering work of Crossley and Burn.[10a,b] However, such acid-catalyzed condensation reactions have been investigated only sporadically thus far.[10,11] Herein, we report a synthetic protocol for quinoline-fused porphyrins through Suzuki–Miyaura coupling of β-borylated porphyrins with 2-iodoaniline and a subsequent Pictet–Spengler cyclization reaction[11,12] of β-2-aminophenylene-substituted porphyrins with aldehydes.

The β-borylated porphyrins $\mathbf{1_{Ni}}$, $\mathbf{5_{Ni}}$, $\mathbf{8_{Ni2}}$, and $\mathbf{11_{Ni}}$ (for structures see Schemes 1–3) were prepared by iridium-catalyzed C–H borylation of meso-unsubstituted porphyrins.[13] Suzuki–Miyaura cross-coupling of $\mathbf{1_{Ni}}$ with 2-iodoaniline under Pd/SPhos[14] catalysis afforded the 2,18-di(2-aminophenyl) $Ni^{II}$/porphyrin $\mathbf{2_{Ni}}$ in 99% yield (Scheme 1). $\mathbf{2_{Ni}}$ was converted into the doubly quinoline-fused porphyrin $\mathbf{3_{Ni}}$ in 78% yield by a Pictet–Spengler cyclization reaction[11,12] with benzaldehyde with the aid of trifluoroacetic acid (TFA). A similar reaction of $\mathbf{2_{Ni}}$ with paraformaldehyde afforded $\mathbf{4_{Ni}}$ in 26% yield. The structures of $\mathbf{3_{Ni}}$ and $\mathbf{4_{Ni}}$ have been unambiguously determined by single-crystal X-ray diffraction analysis (Figure 1). $\mathbf{3_{Ni}}$ takes on a considerably bent conformation as indicated by the large mean-plane deviation (MPD)[15] of 0.345 Å. In contrast, $\mathbf{4_{Ni}}$ takes on a less bent structure with a MPD of 0.275 Å. The larger MPD value of $\mathbf{3_{Ni}}$ can be

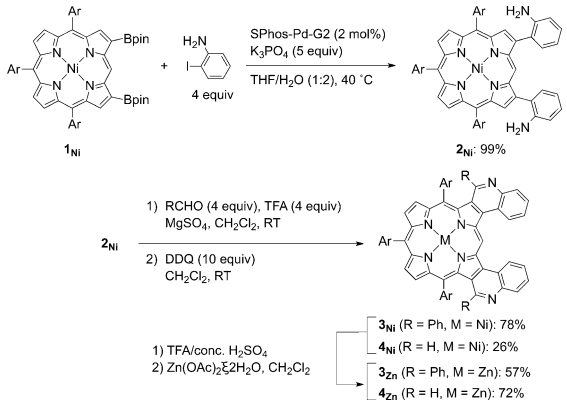


***Scheme 1.*** Synthesis of doubly quinoline-fused porphyrins. Ar = 3,5-di-*tert*-butylphenyl, THF = tetrahydrofuran, DDQ = 2,3-dichloro-5,6-dicyano-1,4-benzoquinone.

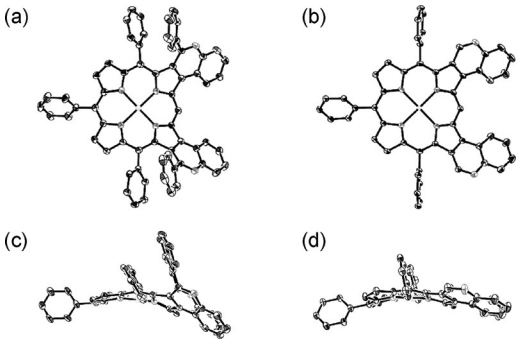


***Figure 1.*** X-ray crystal structures. Top views of $\mathbf{3_{Ni}}$ (a) and $\mathbf{4_{Ni}}$ (b) and side views of $\mathbf{3_{Ni}}$ (c) and $\mathbf{4_{Ni}}$ (d). Thermal ellipsoids are shown at 50% probability. Solvent molecules, *tert*-butyl groups, and all hydrogen atoms are omitted for clarity.

[*] Dr. K. Gao, N. Fukui, Prof. Dr. H. Yorimitsu, Prof. Dr. A. Osuka
Department of Chemistry, Graduate School of Science
Kyoto University, Sakyo-ku, Kyoto 606-8502 (Japan)
E-mail: yori@kuchem.kyoto-u.ac.jp
osuka@kuchem.kyoto-u.ac.jp
S. I. Jung, Prof. Dr. D. Kim
Spectroscopy Laboratory for Functional π-Electronic Systems and Department of Chemistry
Yonsei University, Seoul 120-749 (Korea)
E-mail: dongho@yonsei.ac.kr

Supporting information for this article can be found under: http://dx.doi.org/10.1002/anie.201606293.

  

ascribed to steric repulsion between the aryl groups on the quinoline segments and those at the nearby meso-position. Both $\mathbf{3}_{Ni}$ and $\mathbf{4}_{Ni}$ were converted into the corresponding $Zn^{II}$/porphyrins $\mathbf{3}_{Zn}$ and $\mathbf{4}_{Zn}$, respectively, in moderate yields by an acid-mediated removal of nickel and subsequent zincation.

As an extension, the 2,8,12,18-tetra(2-aminophenyl)porphyrin $\mathbf{6}_{Ni}$ was prepared from the corresponding tetraborylated $Ni^{II}$/porphyrin $\mathbf{5}_{Ni}$ and was then converted into the quadruply quinoline-fused $Ni^{II}$/porphyrin $\mathbf{7}_{Ni}$ in 68% yield (Scheme 2). Moreover, the meso–meso linked porphyrin

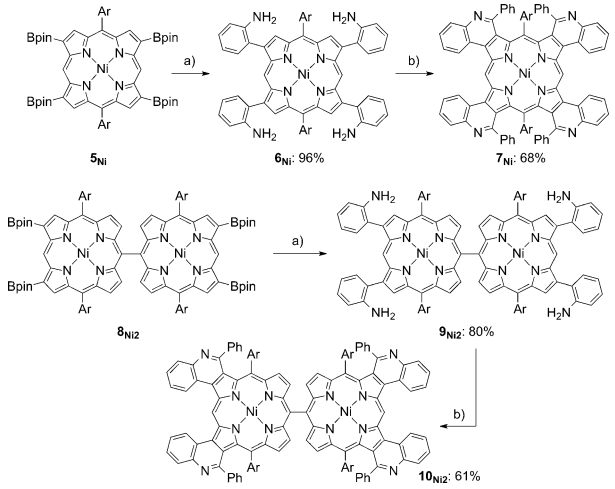


***Scheme 2.*** Synthesis of quadruply quinoline-fused porphyrins. Ar = 3,5-di-*tert*-butylphenyl. Reaction conditions: a) 2-iodoaniline (10 equiv), SPhos-Pd-G2 (2 mol%), $K_3PO_4$ (15 equiv for $\mathbf{5}_{Ni}$, 20 equiv for $\mathbf{8}_{Ni2}$), THF/$H_2O$ (1:2), 40°C; b) Benzaldehyde (8 equiv for $\mathbf{6}_{Ni}$, 16 equiv for $\mathbf{9}_{Ni2}$), TFA (8 equiv for $\mathbf{6}_{Ni}$, 16 equiv for $\mathbf{9}_{Ni2}$), $MgSO_4$, $CH_2Cl_2$, RT, then, DDQ (20 equiv).

dimer $\mathbf{8}_{Ni2}$ was transformed into the quadruply quinoline-fused meso–meso linked porphyrin dimer $\mathbf{10}_{Ni2}$. The X-ray diffraction analysis of $\mathbf{10}_{Ni2}$ showed that each porphyrin unit takes on a bent structure with an MPD of 0.395 and 0.318 Å, respectively, as observed in $\mathbf{3}_{Ni}$. The two porphyrins in $\mathbf{10}_{Ni2}$ are almost perpendicular to each other with a dihedral angle of 80.6° (Figure 2).

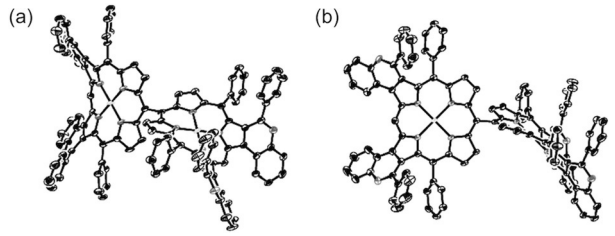


***Figure 2.*** X-ray crystal structure of $\mathbf{10}_{Ni2}$. a) Top view and b) side view. Thermal ellipsoids are shown at 50% probability. Solvent molecules, *tert*-butyl groups, and all hydrogen atoms are omitted for clarity.

This synthetic protocol has been further extended to the synthesis of phenanthroline-fused porphyrin dimers (Scheme 3). Suzuki–Miyaura cross-coupling reaction of the 2-borylated $Ni^{II}$/porphyrin $\mathbf{11}_{Ni}$[13b] with 2,3-diamino-1,4-dibromobenzene in a 2.5:1 ratio provided the β-to-β 1,4-(2,3-diamino)phenylene-bridged $Ni^{II}$/porphyrin dimer $\mathbf{12}_{Ni2}$ in 82% yield. The condensation of $\mathbf{12}_{Ni2}$ with benzaldehyde under similar reaction conditions provided the phenanthroline-fused $Ni^{II}$/porphyrin dimer $\mathbf{13}_{Ni2}$ in 58% yield. Interestingly, the β-to-β 4,7-benzimidazole-bridged porphyrin dimer $\mathbf{14}_{Ni2}$ was formed in 89% yield when the condensation reaction was conducted open to air. The structure of $\mathbf{13}_{Ni2}$ has been determined by X-ray diffraction analysis as shown in Figure 3. Owing to the fused-phenanthroline bridge, the two

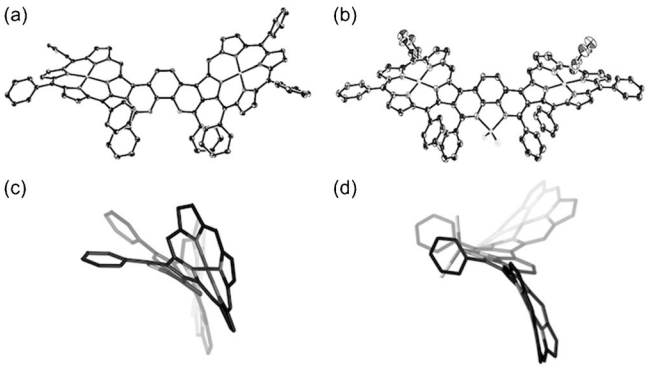


***Figure 3.*** X-ray structures. Top views of $\mathbf{13}_{Ni2}$ (a) and $\mathbf{13}_{Ni2Ni}$ (b) and side views of $\mathbf{13}_{Ni2}$ (c) and $\mathbf{13}_{Ni2Ni}$ (d). Thermal ellipsoids are shown at 50% probability. Structures in (c) and (d) are shown in wire frame model for clarity. Solvent molecules, *tert*-butyl groups, and all hydrogen atoms are omitted for clarity.

units are held in a coplanar manner with a substantial molecular twist. The MPDs of the two porphyrin units are 0.365 and 0.289 Å, and the average dihedral angle between the two $Ni^{II}$/porphyrins is 34.4°. Similarly to $\mathbf{3}_{Ni}$, $\mathbf{13}_{Ni2}$ was transformed into the dimer $\mathbf{13}_{Zn2}$ in 90% yield by demetalation and subsequent zincation.

Since phenanthroline is known to serve as a bidentate ligand for metal ions, we examined the reactions of $\mathbf{13}_{Ni2}$ with metal salts such as $NiCl_2 \cdot 6H_2O$ and $ZnCl_2$. Treatment of these dimers with the metal salts followed by precipitation gave the corresponding trimetallic complexes $\mathbf{13}_{Ni2Ni}$ (82%) and $\mathbf{13}_{Ni2Zn}$ (68%). Similarly, metalation of $\mathbf{13}_{Zn2}$ with $ZnCl_2$ afforded $\mathbf{13}_{Zn2Zn}$ in 98% yield. These trimetallic complexes exhibited the parent ion peaks at the expected positions: *m*/*z* 2229.99 for $\mathbf{13}_{Ni2Ni}$ (calcd for $C_{144}H_{152}{}^{35}ClN_{10}{}^{58}Ni_3$, *m*/*z* 2229.99 $[M-Cl]^+$), *m*/*z* 2236.06 for $\mathbf{13}_{Ni2Zn}$ (calcd for $C_{144}H_{152}{}^{35}ClN_{10}{}^{58}Ni_2{}^{64}Zn$, *m*/*z* 2235.99 $[M-Cl]^+$), and *m*/*z* 2247.93 for $\mathbf{13}_{Zn2Zn}$ (calcd for $C_{144}H_{152}{}^{35}ClN_{10}{}^{64}Zn_3$, *m*/*z* 2247.98 $[M-Cl]^+$). Figure 3 shows the structure of $\mathbf{13}_{Ni2Ni}$, which is more twisted compared with that of $\mathbf{13}_{Ni2}$, as indicated by the dihedral angle (97.7°) between the two $Ni^{II}$/porphyrins. The two porphyrin units are crystallographically equivalent with the MPD of 0.303 Å.

Figure 4a shows the UV/Vis absorption spectra of $\mathbf{2}_{Ni}$, $\mathbf{3}_{Ni}$, $\mathbf{4}_{Ni}$, $\mathbf{7}_{Ni}$, and $\mathbf{10}_{Ni2}$ in $CH_2Cl_2$. The nonfused $Ni^{II}$/porphyrin $\mathbf{2}_{Ni}$ shows a Soret band at $\lambda = 420$ nm and Q-bands at $\lambda = 530$ and 556 nm, while $\mathbf{3}_{Ni}$ displays a Soret

  

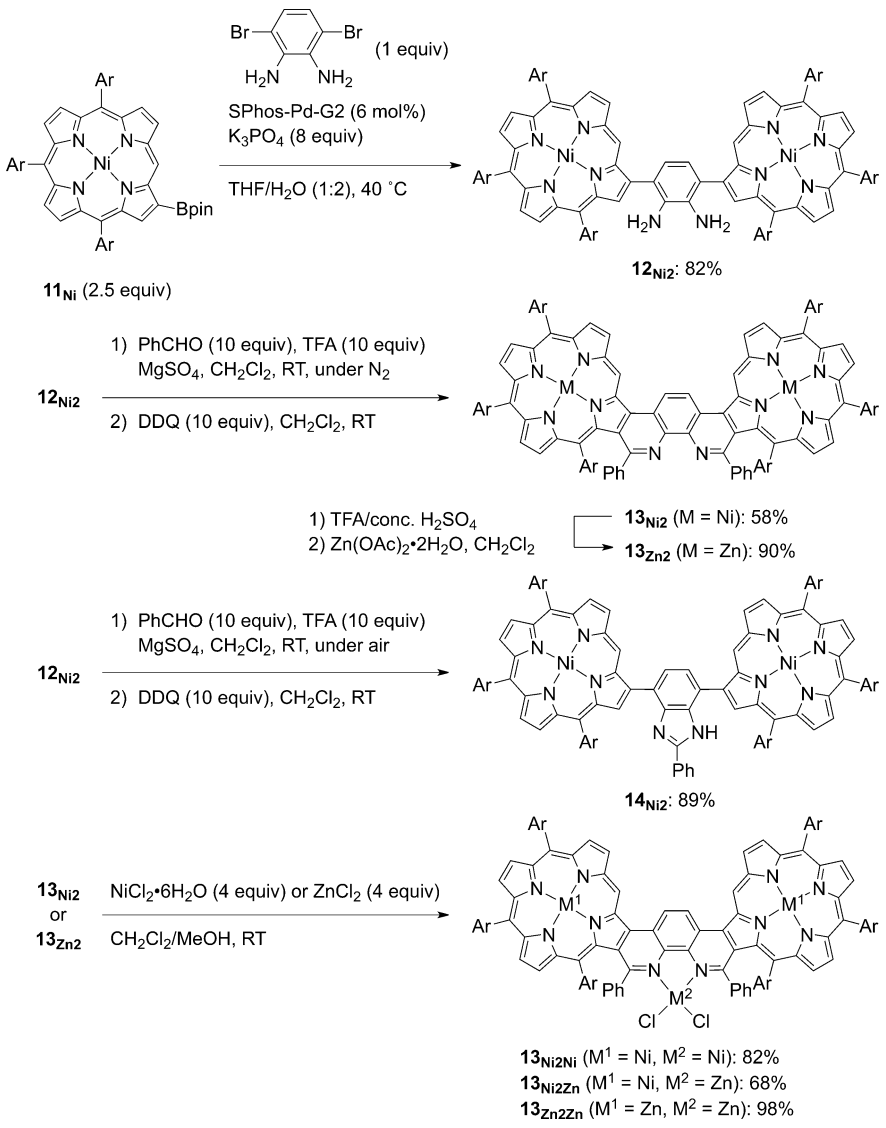


***Scheme 3.*** Synthesis of phenanthroline-bridged diporphyrins. Ar = 3,5-di-*tert*-butylphenyl.

band at $\lambda = 462$ nm and Q-bands at $\lambda = 576$ and 618 nm, and $\mathbf{4_{Ni}}$ displays a Soret band at $\lambda = 447$ nm and Q-bands at $\lambda = 558$ and 596 nm. The more red-shifted absorption bands of $\mathbf{3_{Ni}}$ can be ascribed to the distorted porphyrin plane resulting from the phenyl groups at the quinoline moieties.[16] The absorption spectrum of $\mathbf{7_{Ni}}$ is even more red-shifted, thus featuring a Soret band at $\lambda = 496$ nm and Q-bands at $\lambda = 660$ and 678 nm. The meso–meso linked $\mathbf{10_{Ni2}}$ exhibited Soret bands at $\lambda = 464$ and 482 nm and Q-bands at $\lambda = 585$ and 637 nm. The split Soret bands can be ascribed to exciton coupling between the two porphyrin units.

Figure 4b shows the absorption spectra of $Ni^{II}$/porphyrin dimers. The dimers $\mathbf{12_{Ni2}}$ and $\mathbf{14_{Ni2}}$ possess similar β-to-β 1,4-phenylene linkages and show similar absorption spectra, thus displaying a Soret band at $\lambda = 416$ nm and Q-bands at $\lambda = 526$ and 557 nm and a Soret band at $\lambda = 417$ nm and Q-bands at $\lambda = 528$ and 563 nm, respectively. The Soret bands are not split but broadened as indicated by their full widths at half maximum, 1794 and 1992 $cm^{-1}$ for $\mathbf{12_{Ni2}}$ and $\mathbf{14_{Ni2}}$, respectively, which are distinctly larger than that (1196 $cm^{-1}$) of the corresponding 5,10,15-triaryl $Ni^{II}$/porphyrin monomer. These broad Soret bands can be ascribed to exciton coupling of the two $Ni^{II}$ porphyrins. The absorption spectrum of $\mathbf{13_{Ni2}}$ displays a red-shifted and more split Soret band at $\lambda = 443$ and 468 nm and Q-bands at $\lambda = 556$ and 593 nm as compared with those of $\mathbf{12_{Ni2}}$ and $\mathbf{14_{Ni2}}$, thus indicating increased electronic interaction. Interestingly, trimetallic complexes $\mathbf{13_{Ni2Ni}}$ and $\mathbf{13_{Ni2Zn}}$ show much red-shifted absorption spectra, thus featuring a Soret band at $\lambda = 479$ nm and Q-bands at $\lambda = 565$ and 621 nm, and a Soret band at $\lambda = 480$ nm and Q-bands at $\lambda = 566$ and 622 nm, respectively. The metal coordination may stabilize the LUMO level to decrease the HOMO–LUMO gap. Characteristically, Q(0,0) bands are more intensified than Q(0,1) bands in $\mathbf{13_{Ni2Ni}}$ and $\mathbf{13_{Ni2Zn}}$. In addition, the absorption spectra of $\mathbf{3_{Ni}}$, $\mathbf{4_{Ni}}$, $\mathbf{10_{Ni2}}$, and $\mathbf{13_{Ni2}}$ were drastically changed upon addition of trifluoroacetic acid (TFA; see Figures S8, S16, S33, and S41 in the Supporting Information), apparently because of protonation at the nitrogen atoms. These results indicate that the protonation also caused perturbation of the electronic properties of these $Ni^{II}$ porphyrins.

Similarly to $\mathbf{3_{Ni}}$ and $\mathbf{4_{Ni}}$, the absorption spectrum of $\mathbf{3_{Zn}}$ is red-shifted as compared with that of $\mathbf{4_{Zn}}$. $\mathbf{3_{Zn}}$ and $\mathbf{4_{Zn}}$ exhibit fluorescence with maxima at $\lambda = 639$ nm and 701 nm and at $\lambda =$ 613 nm and 671 nm, respectively. Fluorescence quantum yields ($\Phi_F$) of $\mathbf{3_{Zn}}$ and $\mathbf{4_{Zn}}$ are 0.022 and 0.029, respectively. $\mathbf{13_{Zn2}}$ displays a clearly split Soret band at $\lambda = 446$ and 478 nm and Q-bands at $\lambda = 573$ and 610 nm. $\mathbf{13_{Zn2}}$ shows fluorescence at 617 nm and 674 nm, respectively. The Stokes shift is small (186 $cm^{-1}$) and the fluorescence quantum yield is 0.036. As observed in the trimetallic complexes $\mathbf{13_{Ni2Ni}}$ and $\mathbf{13_{Ni2Zn}}$, $\mathbf{13_{Zn2Zn}}$ also displayed red-shifted absorption and fluorescence spectra with a relatively high fluorescence quantum yield of 0.042, compared to those of $\mathbf{13_{Zn2}}$. The increased fluorescence quantum yield can be ascribed to the rigid structure fixed by Zn metalation. By using a time-correlated single photon counting technique, we have measured fluorescence lifetimes: 1.8 ns, 1.6 ns, and 1.4 ns for $\mathbf{3_{Zn}}$, $\mathbf{4_{Zn}}$, and $\mathbf{13_{Zn2}}$, respectively.

The electrochemical properties of $\mathbf{3_{Ni}}$, $\mathbf{4_{Ni}}$, $\mathbf{7_{Ni}}$, and $\mathbf{13_{Ni2}}$ were examined by cyclic voltammetry (CV; see Table S1). $\mathbf{3_{Ni}}$ showed two reversible oxidation waves at 0.76 and 0.47 V and three reversible reduction waves at −1.62, −1.96, and −2.09 V, while $\mathbf{4_{Ni}}$ showed two reversible oxidation waves at

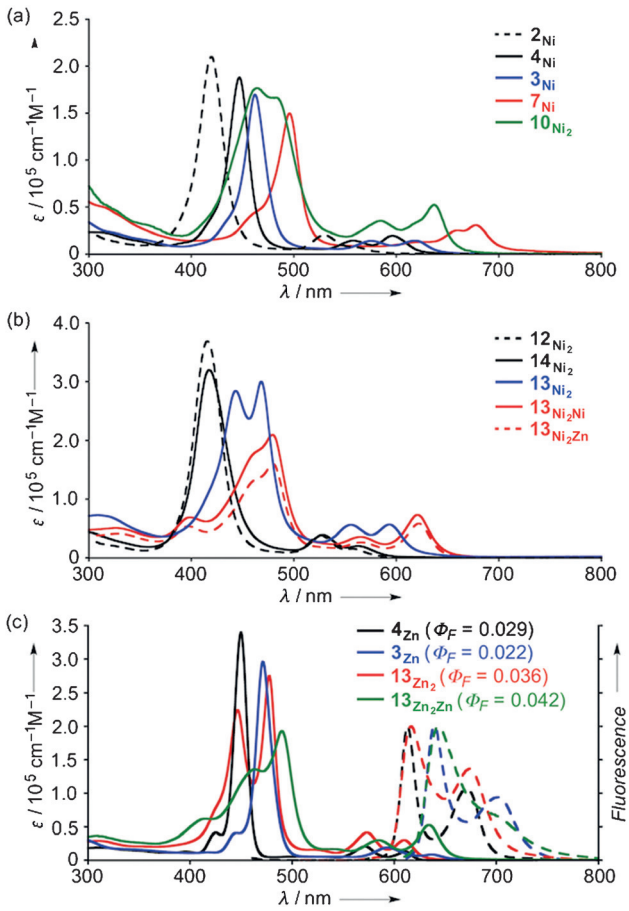


***Figure 4.*** a) UV/Vis absorption spectra of porphyrin monomers $\mathbf{2}_{Ni}$, $\mathbf{3}_{Ni}$, $\mathbf{4}_{Ni}$, $\mathbf{7}_{Ni}$, and $\mathbf{10}_{Ni2}$ in $CH_2Cl_2$. b) UV/Vis absorption spectra of porphyrin dimers $\mathbf{12}_{Ni2}$, $\mathbf{13}_{Ni2}$, $\mathbf{14}_{Ni2}$, $\mathbf{13}_{Ni2Ni}$, and $\mathbf{13}_{Ni2Zn}$ in $CH_2Cl_2$. c) UV/Vis absorption (solid line) and emission (dashed line) spectra of $Zn^{II}$ complexes $\mathbf{3}_{Zn}$, $\mathbf{4}_{Zn}$, $\mathbf{13}_{Zn2}$, and $\mathbf{13}_{Zn2Zn}$ in $CH_2Cl_2$.

0.88 and 0.56 V and two reversible reduction waves at −1.57 and −2.08 V. The observed electrochemical HOMO–LUMO gap of $\mathbf{3}_{Ni}$ (2.09 eV) is slightly smaller than that of $\mathbf{4}_{Ni}$ (2.13 eV), and is consistent with the smaller optical HOMO–LUMO gap of $\mathbf{3}_{Ni}$ as compared with that of $\mathbf{4}_{Ni}$. $\mathbf{7}_{Ni}$ showed two reversible oxidation waves at 0.91 and 0.45 V and two reversible reduction potentials at −1.47 and −1.86 V and hence the electrochemical HOMO–LUMO gap of 1.92 eV. The phenanthroline-bridged dimer $\mathbf{13}_{Ni2}$ showed two reversible oxidation waves and one reversible reduction wave at 0.90, 0.48, and −1.73 V.

The molecular orbitals of meso-free $Ni^{II}$/porphyrin, $\mathbf{3}_{Ni}$, $\mathbf{4}_{Ni}$, $\mathbf{13}_{Ni2}$, and $\mathbf{13}_{Ni2Ni}$ have been examined by density functional theory (DFT) calculations at the B3LYP/6-31G*-(C,H,N) + LANL2DZ(Ni) level using the Gaussian 09 package (see Figures S71–S76).[17] Compared to meso-free $Ni^{II}$/porphyrin, $\mathbf{3}_{Ni}$ and $\mathbf{4}_{Ni}$ showed stabilized LUMOs resulting from the electron-accepting fused quinoline moieties. The calculated HOMO–LUMO gap of $\mathbf{3}_{Ni}$ (−2.65 eV), which is smaller than that of $\mathbf{4}_{Ni}$ (−2.73 eV), accords with the optical and electrochemical measurements. Coordination of $\mathbf{13}_{Ni2}$ to Lewis-acidic $Ni^{II}$ significantly lowered the LUMO level from −2.24 eV to −2.67 eV, and it is also consistent with the experimental results.

In summary, we have developed a concise protocol to synthesize quinoline-fused porphyrins and phenanthroline-bridged porphyrin dimers by Pictet–Spengler synthesis. Construction of peri-fused electron-accepting quinoline units caused red-shifted absorption spectra and higher reduction potentials. In addition, such external pyridine units also act as a coordination site, and the metalation of $\mathbf{13}_{Ni2}$ led to the increased structural distortion and largely altered absorption. Further investigation on the synthesis of more elaborate π-extended porphyrins is underway in our laboratory.

## Acknowledgments

This work was supported by Grants-in-Aid for Scientific Research from MEXT (Nos.: 25107002 (“Science of Atomic Layers”), 16H01019 (“Precisely Designed Catalysts with Customized Scaffolding”), 16H01149 (“Middle Molecular Strategy”)) and from JSPS (Nos.: 25220802 (Scientific Research (S)), 16H04109 (B), 24685007 (Young Scientists (A)) and 26620081 (Exploratory Research)). K.G. acknowledges a JSPS Postdoctoral Fellowship for Foreign Researchers. N.F. acknowledges a JSPS Fellowship for Young Scientists. H.Y. acknowledges Kansai Research Foundation for Technology Promotion and Asahi Glass Foundation for financial support. The work in Korea was supported by Global Research Laboratory 2013K1A1A2A02050183.

**Keywords:** heterocycles · nickel · porphyrinoids · supramolecular chemistry · zinc

**How to cite:** *Angew. Chem. Int. Ed.* **2016**, *55*, 13038–13042
*Angew. Chem.* **2016**, *128*, 13232–13236

[1] a) H. Mori, T. Tanaka, A. Osuka, *J. Mater. Chem. C* **2013**, *1*, 2500; b) T. Tanaka, A. Osuka, *Chem. Soc. Rev.* **2015**, *44*, 943; c) J. P. Lewtak, D. Gryko, *Chem. Commun.* **2012**, *48*, 10069.
[2] a) A. Tsuda, A. Osuka, *Science* **2001**, *293*, 79; b) N. K. S. Davis, A. L. Thompson, H. L. Anderson, *J. Am. Chem. Soc.* **2011**, *133*, 30; c) K. Naoda, H. Mori, N. Aratani, B. S. Lee, D. Kim, A. Osuka, *Angew. Chem. Int. Ed.* **2012**, *51*, 9856; *Angew. Chem.* **2012**, *124*, 9994; d) H. Mori, T. Tanaka, S. Lee, J. M. Lim, D. Kim, A. Osuka, *J. Am. Chem. Soc.* **2015**, *137*, 2097.
[3] a) H. Imahori, T. Umeyama, S. Ito, *Acc. Chem. Res.* **2009**, *42*, 1809; b) M. Tanaka, S. Hayashi, S. Eu, T. Umeyama, Y. Matano, H. Imahori, *Chem. Commun.* **2007**, 2069; c) J. M. Ball, N. K. S. Davis, J. D. Wilkinson, J. Kirkpatrick, J. Teuscher, R. Gunning, H. L. Anderson, H. J. Snaith, *RSC Adv.* **2012**, *2*, 6846.
[4] a) T. K. Ahn, K. S. Kim, D. Y. Kim, S. B. Noh, N. Aratani, C. Ikeda, A. Osuka, D. Kim, *J. Am. Chem. Soc.* **2006**, *128*, 1700; b) S. Baluschev, V. Yakutkin, T. Miteva, Y. Avlasevich, S. Chernov, S. Aleschenkov, G. Nelles, A. Cheprakov, A. Yasuda, K. Müllen, G. Wegner, *Angew. Chem. Int. Ed.* **2007**, *46*, 7693; *Angew. Chem.* **2007**, *119*, 7837; c) M. K. Kuimova, S. W. Botchway, A. W. Parker, M. Balaz, H. A. Collins, H. L. Anderson, K. Suhling, P. R. Ogilby, *Nat. Chem.* **2009**, *1*, 69.
[5] C. Borek, K. Hanson, P. J. Djurovich, M. E. Thompson, K. Aznavour, R. Bau, Y. Sun, S. R. Forrest, J. Brooks, L. Michalski, J. Brown, *Angew. Chem. Int. Ed.* **2007**, *46*, 1109; *Angew. Chem.* **2007**, *119*, 1127.

  

[6] a) K. Kurotobi, K. S. Kim, S. B. Noh, D. Kim, A. Osuka, *Angew. Chem. Int. Ed.* **2006**, *45*, 3944; *Angew. Chem.* **2006**, *118*, 4048; b) M. Akita, S. Hiroto, H. Shinokubo, *Angew. Chem. Int. Ed.* **2012**, *51*, 2894; *Angew. Chem.* **2012**, *124*, 2948; c) N. Fukui, W.-Y. Cha, S. Lee, S. Tokuji, D. Kim, H. Yorimitsu, A. Osuka, *Angew. Chem. Int. Ed.* **2013**, *52*, 9728; *Angew. Chem.* **2013**, *125*, 9910; d) W. Zeng, B. S. Lee, Y. M. Sung, K.-W. Huang, Y. Li, D. Kim, J. Wu, *Chem. Commun.* **2012**, *48*, 7684.

[7] a) S. Fox, R. W. Boyle, *Chem. Commun.* **2004**, 1322; b) T. Ishizuka, Y. Saegusa, Y. Shiota, K. Ohtake, K. Yoshizawa, T. Kojima, *Chem. Commun.* **2013**, *49*, 5939; c) Y. Mitsushige, S. Yamaguchi, B. S. Lee, Y. M. Sung, S. Kuhri, C. A. Shierl, D. M. Guldi, D. Kim, Y. Matsuo, *J. Am. Chem. Soc.* **2012**, *134*, 16540.

[8] a) Y. Lin, T. D. Lash, *Tetrahedron Lett.* **1995**, *36*, 9441; b) T. D. Lash, V. Gandhi, *J. Org. Chem.* **2000**, *65*, 8020; T. D. Lash, Y. Lin, B. H. Noval, M. Parikh, *Tetrahedron* **2005**, *61*, 11601.

[9] a) S. Ito, T. Murashima, N. Ono, *J. Chem. Soc. Perkin Trans. 1* **1997**, 3161; b) S. Ito, T. Murashima, H. Uno, N. Ono, *Chem. Commun.* **1998**, 1661; c) Y. Inokuma, N. Ono, H. Uno, D. Y. Kim, S. B. Noh, D. Kim, A. Osuka, *Chem. Commun.* **2005**, 3782.

[10] a) M. Crossley, P. L. Burn, *J. Chem. Soc. Chem. Commun.* **1987**, 39; b) M. Crossley, P. L. Burn, *J. Chem. Soc. Chem. Commun.* **1991**, 1569; c) S. Tokuji, Y. Takahashi, H. Shinmori, H. Shinokubo, A. Osuka, *Chem. Commun.* **2009**, 1028; d) S. Richeter, A. H. Aissa, C. Taffin, A. van der Lee, D. Leclercq, *Chem. Commun.* **2007**, 2148.

[11] D. K. Singh, M. Nath, *Org. Biomol. Chem.* **2015**, *13*, 1836.

[12] a) A. Pictet, T. Spengler, *Ber. Dtsch. Chem. Ges.* **1911**, *44*, 2030; b) E. D. Cox, J. M. Cook, *Chem. Rev.* **1995**, *95*, 1797.

[13] a) H. Hata, H. Shinokubo, A. Osuka, *J. Am. Chem. Soc.* **2005**, *127*, 8264; b) H. Hata, S. Yamaguchi, G. Mori, S. Nakazono, T. Katoh, K. Takatsu, S. Hiroto, H. Shinokubo, A. Osuka, *Chem. Asian J.* **2007**, *2*, 849.

[14] 2-(2′,6′-Dimethoxybiphenyl)dicyclohexylphosphine: T. E. Barder, S. D. Walker, J. R. Martinelli, S. L. Buchwald, *J. Am. Chem. Soc.* **2005**, *127*, 4685.

[15] MPDs are defined by the 25 core atoms consisting of meso-carbon atoms, four pyrrole units, and a central nickel atom.

[16] R. E. Haddad, S. Gazeau, J. Pécaut, J. C. Marchon, C. J. Medforth, J. A. Shelnutt, *J. Am. Chem. Soc.* **2003**, *125*, 1253.

[17] M. J. Frisch, et al., Gaussian 09, Revision C.02; Gaussian, Inc., Wallingford, CT, **2009**.

Received: June 29, 2016
Revised: August 25, 2016
Published online: September 16, 2016

  